Archive of Applied Mechanics 71 (2001) 43–52 © Springer-Verlag 2001

(3)

Variation of the stress intensity factor along the crack front of interacting semi-elliptical surface cracks

N.-A. Noda, K. Kobayashi, T. Oohashi

Summary In this study, the interaction between two semi-elliptical co-planar surface cracks is considered when Poisson's ratio $\nu = 0.3$. The problem is formulated as a system of singular integral equations, based on the idea of the body force method. In the numerical calculation, the unknown density of body force density is approximated by the product of a fundamental density function and a polynomial. The results show that the present method yields smooth variations of stress intensity factors along the crack front very accurately, for various geometrical conditions. When the size of crack 1 is larger than the size of crack 2, the maximum stress intensity factor appears at a certain point, $\beta_1 = 177°$, of crack 1. Along the outside of crack 1, that is at $\beta_1 = 0 \sim 90°$, the interaction can be negligible even if the two cracks are very close. The interaction can be negligible when the two cracks are spaced in such a manner that their two closest points are separated by a distance exceeding the small crack's major diameter. The variations of stress intensity factor of a semi-elliptical crack are tabulated and charted.

Key words Elasticity, stress intensity factor, body force method, semi-elliptical surface crack, interaction, singular integral equation

1 Introduction

Elliptical and semi-elliptical three-dimensional (3D) cracks are fundamental and useful in evaluating the strength of structures and engineering materials. However, it is difficult to determine smooth variation of the stress intensity factor (SIF) along the front of a 3D surface crack. In previous studies, interaction between 3D cracks was considered by using FEM analysis, [1–3] and by an alternative method, [4]. The interaction of two semi-elliptical cracks was also considered by using the body force method, when Poisson's ratio $\nu = 0$, [5, 6]. Recently, in order to analyze such 3D cracks accurately, the body force method, [7, 8], has been widely applied due to its efficiency, [9, 10]. However, to obtain a smooth distribution of the SIF is especially difficult for the practical case of $\nu = 0.3$, because the SIF rapidly changes near the free surface, [11–13].

In a preceding paper, numerical solutions of the singular integral equation of the body force method in a single 3D crack has been discussed, [14]. Unknown body force densities were approximated by the products of fundamental density functions and polynomials. The results showed that the analytical method yields a smooth variation of the SIF with a higher accuracy as compared to other methods. In this study, the method will be applied to the interaction between two semi-elliptical cracks when $\nu = 0.3$. With varying of the spacing and the shape of the ellipse, the variation of the SIF will be discussed.

Received 30 August 1999; accepted for publication 22 February 2000

N.-A. Noda, K. Kobayashi, T. Oohashi
Department of Mechanical Engineering,
Kyushu Institute of Technology,
Kitakyushu 804-8550, Japan

The authors wish to express their thanks to the members of their group, especially Mr. T. Kihara, who carried out much of the computational work.

2
Theory and solution

Consider a semi-infinite body under uniform tension containing two semi-elliptical cracks as shown in Fig. 1. Here, the xz-plane is free from stress, and the two semi-elliptical cracks, whose principal diameters are $(2a_1, 2b_1)$ and $(2a_2, 2b_2)$, are embedded in the xy-plane. The body force method is used to formulate the problem as a system of singular integral equations, whose unknowns are densities of body forces $f_1(\xi_1, \eta_1)$ and $f_2(\xi_2, \eta_2)$. Here, (ξ_i, n_i, ζ_i) is a (x_i, y_i, z_i) coordinate of the point where the body force is applied at the i-th crack. The body force density is equivalent to a crack opening displacement $U_z(x_a, y_b)$, [15],

$$\begin{aligned}
-\sigma_z^\infty &= \frac{H}{2\pi}\left[\iint\limits_{S_1} \frac{f_1(\xi_1,\eta_1)}{r_1^3}\mathrm{d}\xi_1\,\mathrm{d}\eta_1 + \iint\limits_{S_1} K_1^{f_1}(\xi_1,\eta_1,x_1,y_1)f_1(\xi_1,\eta_1)\mathrm{d}\xi_1\,\mathrm{d}\eta_1 .\right. \\
&\quad \left. + \iint\limits_{S_2}\left\{\frac{1}{r_3^3} + K_1^{f_2}(\xi_2,\eta_2,x_1,y_1)\right\}f_1(\xi_1,\eta_1)\mathrm{d}\xi_2\,\mathrm{d}\eta_2\right], \\
-\sigma_z^\infty &= \frac{H}{2\pi}\left[\iint\limits_{S_2} \frac{f_2(\xi_2,\eta_2)}{r_5^3}\mathrm{d}\xi_2\,\mathrm{d}\eta_2 + \iint\limits_{S_2} K_2^{f_2}(\xi_2,\eta_2,x_2,y_2)f_2(\xi_2,\eta_2)\mathrm{d}\xi_2\,\mathrm{d}\eta_2 .\right. \\
&\quad \left. + \iint\limits_{S_1}\left\{\frac{1}{r_7^3} + K_2^{f_1}(\xi_1,\eta_1,x_2,y_2)\right\}f_1(\xi_1,\eta_1)\mathrm{d}\xi_1\,\mathrm{d}\eta_1\right],
\end{aligned} \tag{1a}$$

where

$$\begin{aligned}
K_1^{f_1}(\xi_1,\eta_1,x_1,y_1) &= \frac{5-20\nu+24\nu^2}{r_2^3} + \frac{12(1-\nu)(1-2\nu)}{r_2(r_2+y_1+\eta_1)} + \frac{6\{3y_1\eta_1 - 2\nu(1-2\nu)(y_1+\eta_1)\}}{r_1^5}, \\
K_1^{f_2}(\xi_2,\eta_2,x_1,y_1) &= \frac{5-20\nu+24\nu^2}{r_4^3} + \frac{12(1-\nu)(1-2\nu)}{r_4(r_4+y_1+\eta_2)} + \frac{6\{3y_1\eta_2 - 2\nu(1-2\nu)(y_1+\eta_2)\}}{r_4^5}, \\
K_2^{f_2}(\xi_2,\eta_2,x_2,y_2) &= \frac{5-20\nu+24\nu^2}{r_6^3} + \frac{12(1-\nu)(1-2\nu)}{r_6(r_6+y_2+\eta_2)} + \frac{6\{3y_2\eta_2 - 2\nu(1-2\nu)(y_2+\eta_2)\}}{r_6^5}, \\
K_2^{f_1}(\xi_1,\eta_1,x_2,y_2) &= \frac{5-20\nu+24\nu^2}{r_8^3} + \frac{12(1-\nu)(1-2\nu)}{r_8(r_8+y_2+\eta_1)} + \frac{6\{3y_2\eta_1 - 2\nu(1-2\nu)(y_2+\eta_1)\}}{r_8^5},
\end{aligned} \tag{1b}$$

$$\begin{aligned}
r_1 &= \sqrt{(x_1-\xi_1)^2+(y_1-\eta_1)^2}, & r_2 &= \sqrt{(x_1-\xi_1)^2+(y_1+\eta_1)^2}, \\
r_3 &= \sqrt{(x_1+d-\xi_2)^2+(y_1-\eta_2)^2}, & r_4 &= \sqrt{(x_1+d-\xi_2)^2+(y_1+\eta_2)^2}, \\
r_5 &= \sqrt{(x_2-\xi_2)^2+(y_2-\eta_2)^2}, & r_6 &= \sqrt{(x_2-\xi_2)^2+(y_2+\eta_2)^2}, \\
r_7 &= \sqrt{(x_2-d-\xi_1)^2+(y_2-\eta_1)^2}, & r_8 &= \sqrt{(x_2-d-\xi_1)^2+(y_2+\eta_1)^2},
\end{aligned} \tag{1c}$$

$$H = \frac{1-2\nu}{4(1-\nu)^2},$$

$$S_1 = \left\{(\xi_1,\eta_1)\left(\frac{\xi_1}{d}\right)^2 + \left(\frac{\eta_1}{b}\right)^2 \le 1, \eta_1 \ge 0\right\}, \quad S_2 = \left\{(\xi_2,\eta_2)\left(\frac{\xi_2}{d}\right)^2 + \left(\frac{\eta_2}{b}\right)^2 \le 1, \eta_2 \ge 0\right\},$$

$$U_z(x_a,y_b) = u_z(x_a,y_b,+0) - u_z(x_a,y_b,-0) = \frac{(1-2\nu)(1+\nu)}{E(1-\nu)}f_{zz}(x_a,y_b) . \tag{1d}$$

Equation (1a) enforces boundary conditions at the prospective boundary S_i for cracks; that is, $\sigma_z = 0$. Equation (1) includes singular terms in the form of $1/r^3, 1/r^5$, corresponding to the

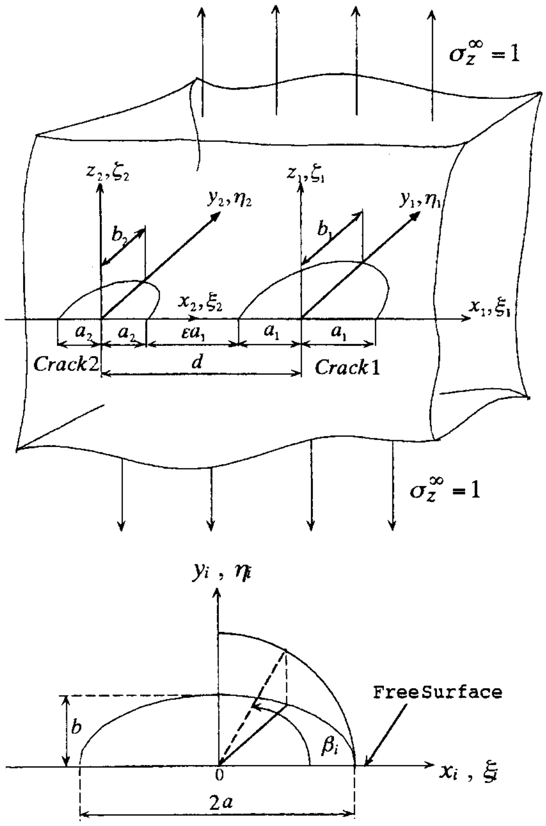

Fig. 1. Two semi-elliptical surface cracks in a semi-infinite body under tension

terms for an elliptical crack in an infinite body. Therefore, the integration should be interpreted in the Hadamard's sense, [16], in the region S_i. The notation $K_1^{f_1}(\xi_1, \eta_1, x_1, y_1)$ refers to a function that satisfies the boundary condition for the free surface, and u_z refers to a displacement in the z direction.

3
Numerical solution of singular integral equations

In the conventional body force method [7, 8], the crack region is divided into several elements, and unknown functions of the body force densities are approximated by using fundamental density functions and step functions. However, the expressions using step functions give rise to singularities along the element boundaries, and they tend to deteriorate the accuracy and validity in sophisticated problems. In the present analysis, the following expressions have been used to approximate the unknown functions as continuous functions. First, we put

$$f_i(\xi_i, \eta_i) = F_i(\xi'_i, \eta'_i) w_i(\xi'_i, \eta'_i),$$

$$w_i(\xi'_i, \eta'_i) = \frac{b_i \sigma_z^\infty}{H\Phi_i} \sqrt{1 - \xi'^2_i - \eta'^2_i},$$

$$\xi'_i = \frac{\xi_i}{a_i}, \eta'_i = \frac{\eta_i}{b_i},$$

$$\Phi_i = \begin{cases} E(k_i), k_i = \sqrt{1 - \left(\dfrac{b_i}{a_i}\right)^2} & (a_i \geq b_i) \\ \dfrac{b_i}{a_i} E(k'_i), k'_i = \sqrt{1 - \left(\dfrac{a_i}{b_i}\right)^2} & (a_i < b_i) \quad i = 1, 2, \end{cases} \tag{2}$$

$$E(k_i) = \int_0^{\pi/2} \sqrt{1 - k_i^2 \sin^2 \lambda} \, d\lambda \ .$$

Here, $w_i(\xi'_i, \eta'_i)$ is called a fundamental density function of the body force, which exactly expresses the stress field due to an elliptical crack in an infinite body under uniform tension σ_z, and leads to solutions with high accuracy. In this calculation, we put $\sigma_z^\infty = 1$. Using expression (2), Eqs. (1) are expressed as

$$
\begin{aligned}
-\sigma_z^\infty = \frac{H}{2\pi}\Bigg[& \iint_{S_1} \frac{F_1(\xi'_1, \eta'_1)}{r_1^3}\sqrt{1-\xi_1'^2-\eta_1'^2}\,\mathrm{d}\xi_1\,\mathrm{d}\eta_1 . \\
& + \iint_{S_1} K_1^{f_1}(\xi_1, \eta_1, x_1, y_1) F_1(\xi'_1, \eta'_1)\sqrt{1-\xi_1'^2-\eta_1'^2}\,\mathrm{d}\xi_1\,\mathrm{d}\eta_1 \\
& + \iint_{S_2} \left\{\frac{1}{r_3^3} + K_1^{f_2}(\xi_2, \eta_2, x_1, y_1)\right\} F_2(\xi'_2, \eta'_2)\sqrt{1-\xi_2'^2-\eta_2'^2}\,\mathrm{d}\xi_2\,\mathrm{d}\eta_2 \Bigg] , \\
-\sigma_z^\infty = \frac{H}{2\pi}\Bigg[& \iint_{S_2} \frac{F_2(\xi'_2, \eta'_2)}{r_5^3}\sqrt{1-\xi_2'^2-\eta_2'^2}\,\mathrm{d}\xi_2\,\mathrm{d}\eta_2 . \\
& + \iint_{S_2} K_2^{f_2}(\xi_2, \eta_2, x_2, y_2) F_2(\xi'_2, \eta'_2)\sqrt{1-\xi_2'^2-\eta_2'^2}\,\mathrm{d}\xi_2\,\mathrm{d}\eta_2 \\
& + \iint_{S_1} \left\{\frac{1}{r_7^3} + K_2^{f_2}(\xi_1, \eta_1, x_2, y_2)\right\} F_1(\xi'_1, \eta'_1)\sqrt{1-\xi_1'^2-\eta_1'^2}\,\mathrm{d}\xi_1\,\mathrm{d}\eta_1 \Bigg] ,
\end{aligned} \tag{3}
$$

whose unknowns are $F_i(\xi'_i, \eta'_i), i = 1, 2$, which are called weight functions.

The following expressions can be applied to approximate unknown functions $F_i(\xi'_i, \eta'_i), i = 1, 2$:

$$
\begin{aligned}
F_1(\xi'_1, \eta'_1) &= \alpha_0 + \alpha_1\eta'_1 + \cdots + \alpha_{n-1}{\eta'_1}^{n-1} + \alpha_n{\eta'_1}^{n} \\
&\quad + \alpha_{n+1}\xi'_1 + \alpha_{n+2}\xi'_1\eta'_1 + \cdots + \alpha_{2n}\xi'_1{\eta'_1}^{n-1} \\
&\quad \vdots \qquad\qquad \vdots \\
&\quad + \alpha_{l-2}{\xi'_1}^{n-1} + \alpha_{l-1}{\xi'_1}^{n-1}\eta'_1 \\
&\quad + \alpha_l{\xi'_1}^{n} \\
&= \sum_{i=0}^{l} \alpha_i G_i(\xi'_i, \eta'_i) ,
\end{aligned} \tag{4a}
$$

where

$$
l = \sum_{k=0}^{n}(k+1) = \frac{(n+1)(n+2)}{2},
$$

$$
G_0(\xi'_1, \eta'_1) = 1, G_1(\xi'_1, \eta'_1) = \eta'_1, \ldots, G_{n+1}(\xi'_1, \eta'_1) = \xi'_1, \ldots, G_l(\xi'_1, \eta'_1) = \xi_1^n,
$$

and

$$
\begin{aligned}
F_2(\xi'_2, \eta'_2) &= \beta_0 + \beta_1\eta'_2 + \cdots + \beta_{n-1}{\eta'_2}^{n-1} + \beta_n{\eta'_2}^{n} \\
&\quad + \beta_{n+1}(-\xi'_2) + \beta_{n+2}(-\xi'_2)\eta'_2 + \cdots + \beta_{2n}(-\xi'_2){\eta'_2}^{n-1} \\
&\quad \vdots \qquad\qquad \vdots \\
&\quad + \beta_{l-2}(-\xi'_2)^{n-1} + \beta_{l-1}(-\xi'_2)^{n-1}\eta'_2 \\
&\quad + \beta_l(-\xi'_2)^{n} \\
&= \sum_{i=0}^{l} \beta_i Q_i(\xi'_2, \eta'_2) ,
\end{aligned} \tag{4b}
$$

where

$$Q_0(\xi_2',\eta_2')=1, Q_1(\xi_2',\eta_2')=\eta_2',\ldots,Q_{n+1}(\xi_2',\eta_2')=(-\xi_2'),\ldots,Q_l(\xi_2',\eta_2')=(-\xi_2')^n \ .$$

Using the approximation method mentioned above, we obtain the following system of algebraic equations for the determination of unknown coefficients α_i, β_i, $i=1,2,\ldots,l$, $l=(1/2)(n+1)(n+2)$, which can be determined by selecting a set of collocation points:

$$\begin{aligned}&\frac{1}{2\pi}\sum_{i=0}^{l}\left[\alpha_i(A_{1,i}^{f_1}+B_{1,i}^{f_1})+\beta_i B_{1,i}^{f_2}\right]=-1,\\&\frac{1}{2\pi}\sum_{i=0}^{l}\left[\alpha_i B_{2,i}^{f_1}+\beta_i(A_{2,i}^{f_2}+B_{2,i}^{f_2})\right]=-1\ ,\end{aligned} \tag{5}$$

The number of unknowns in Eqs. (5) is $2(l+1)$. The notations $A_{1,i}^{f_1}, B_{1,i}^{f_1}, B_{1,i}^{f_2}, B_{2,i}^{f_1}, A_{2,i}^{f_2}, B_{2,i}^{f_2}$ are expressed by

$$\begin{aligned}A_{1,i}^{f_1}&=\frac{b_1}{\Phi_1}\iint\limits_S\frac{G_i(\xi_1',\eta_1')}{r_1^3}\sqrt{1-\xi_1'^2-\eta_1'^2}\,\mathrm{d}\xi_1\,\mathrm{d}\eta_1,\\B_{1,i}^{f_1}&=\frac{b_1}{\Phi_1}\iint\limits_S K_1^{f_1}(\xi_1,\eta_1,x_1,y_1)G_i(\xi_1',\eta_1')\sqrt{1-\xi_1'^2-\eta_1'^2}\,\mathrm{d}\xi_1\,\mathrm{d}\eta_1,\\B_{1,i}^{f_2}&=\frac{b_2}{\Phi_2}\iint\limits_S\left\{\frac{1}{r_3^3}+K_1^{f_2}(\xi_2,\eta_2,x_1,y_1)\right\}Q_i(\xi_2',\eta_2')\sqrt{1-\xi_2'^2-\eta_2'^2}\,\mathrm{d}\xi_2\,\mathrm{d}\eta_2,\\B_{2,i}^{f_1}&=\frac{b_1}{\Phi_1}\iint\limits_S\left\{\frac{1}{r_7^3}+K_2^{f_2}(\xi_1,\eta_1,x_2,y_2)\right\}G_i(\xi_1',\eta_1')\sqrt{1-\xi_1'^2-\eta_1'^2}\,\mathrm{d}\xi_1\,\mathrm{d}\eta_1,\\A_{2,i}^{f_2}&=\frac{b_2}{\Phi_2}\iint\limits_S\frac{Q_i(\xi_2',\eta_2')}{r_5^3}\sqrt{1-\xi_2'^2-\eta_2'^2}\,\mathrm{d}\xi_2\,\mathrm{d}\eta_2,\\B_{2,i}^{f_2}&=\frac{b_2}{\Phi_2}\iint\limits_S K_1^{f_1}(\xi_2,\eta_2,x_2,y_2)Q_i(\xi_2',\eta_2')\sqrt{1-\xi_2'^2-\eta_2'^2}\,\mathrm{d}\xi_2\,\mathrm{d}\eta_2\ .\end{aligned} \tag{6}$$

In Eqs. (6), $A_{1,i}^{f_1}$ and $A_{2,i}^{f_2}$ cannot be evaluated by ordinary numerical procedure because they have hypersingularites of the form r^{-3}. They can be evaluated in the similar way as in [14, 17]. Figure 2 indicates boundary collocation points. In the (x_i',y_i')-plane, where $x_i'=x_i/a_i, y_i'=y_i/b_i$, the boundary conditions are considered at the intersection of the mesh whose interval is 0.02 within the region $x^2+y^2\le 1$ and $y\ge 0$. On the line $y'=0$, some integrals in Eq. (6) cannot be calculated; then, the boundary conditions are considered on the line $y'=0.015$ instead of $y'=0$. In solving the algebraic Eq. (5), the least-square regression method is applied to minimize the residual of stresses at the collocation points.

4
Numerical results and discussion

Numerical calculations have been carried out at changing n in Eqs. (4) for $b_i/a_i=0.5, 1.0$. The Poisson's ratio is assumed to be 0.3. Numerical integrals have been performed using scientific subroutine library (FACOM SSL II DAQE etc.). The convergence of the results and compliance of the boundary conditions are considered in a similar way as in [14]. It is found that when $n=25$, the values of $F_{Ii}(\beta_i)$ have good convergence to the third digit, and the remaining stress σ_z is less than 3×10^{-3} throughout the crack surface. However, it should be noted that the singularity changes its order at the free surface, [11–13], and the numerical values of the SIF may be not reliable at $\beta_1=0$ and 180°. In demonstrating the numerical results of the SIF $K_{Ii}(\beta_i)$, the following dimensionless factor $F_{Ii}(\beta_i)$ will be used:

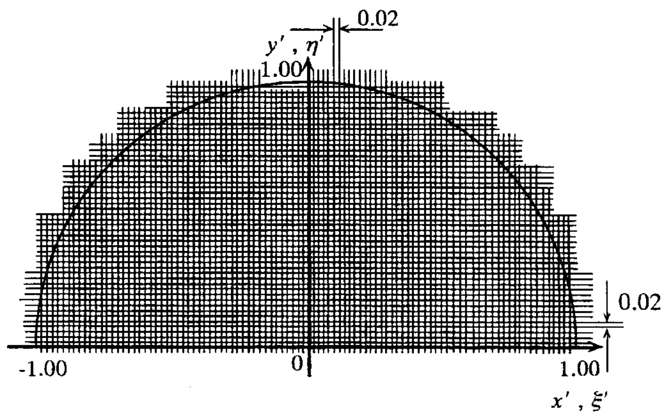

Fig. 2. Boundary collocation points

$$F_{Ii}(\beta_i) = \frac{K_{Ii}(\beta_i)}{\sigma_z^\infty\sqrt{\pi b_i}} = \frac{F_i(\xi_i', \eta_i')|_{\xi_i'=\cos\beta_i, \eta_i'=\sin\beta_i}}{\Phi}\left[\sin^2\beta_i + \left(\frac{b_i}{a_i}\right)^2\cos^2\beta_i\right]^{1/4} . \quad (7)$$

4.1 Two identical cracks ($a_1 = a_2, b_1 = b_2$ in Fig. 1)

Table 1 gives the values of $F_{Ii}(\beta_i)$ for two identical cracks. The results for a single semi-elliptical crack, [12], are indicated in Table 1 as $\lambda = 2a_1/d \to 0$. Figure 3 is a plot of the results of Table 1. The maximum SIF appears at $\beta_1 = 177°$, similarly to the case of a single crack. Figure 4 shows the interaction factor defined as

Table 1. Values of $F_{Ii}(\beta_i)$ of two identical semi-elliptical cracks, $F_{Ii}(\beta_i) = K_{Ii}(\beta_i)/\sigma_z^\infty\sqrt{\pi b_i}$

β_1 (°) \ λ	0	0.667	0.800	0.887	0.900
(a) $b_1/a_1 = b_2/a_2 = 1$					
1	0.742	0.748	0.751	0.755	0.755
2	0.746	0.752	0.755	0.759	0.759
3	0.748	0.754	0.757	0.761	0.761
4	0.746	0.752	0.755	0.759	0.759
5	0.742	0.748	0.751	0.754	0.755
6	0.738	0.743	0.747	0.750	0.751
7	0.733	0.738	0.742	0.745	0.746
8	0.729	0.734	0.738	0.741	0.742
9	0.725	0.730	0.734	0.737	0.738
10	0.721	0.726	0.730	0.733	0.734
15	0.708	0.713	0.716	0.720	0.720
30	0.682	0.687	0.690	0.694	0.694
45	0.669	0.674	0.678	0.681	0.682
60	0.663	0.668	0.672	0.675	0.676
75	0.659	0.665	0.669	0.673	0.674
90	0.659	0.665	0.670	0.675	0.676
105	0.659	0.667	0.673	0.680	0.682
120	0.663	0.672	0.681	0.691	0.693
135	0.669	0.681	0.694	0.711	0.713
150	0.682	0.697	0.717	0.745	0.750
165	0.708	0.727	0.754	0.802	0.813
170	0.721	0.741	0.771	0.826	0.838
171	0.725	0.745	0.776	0.831	0.844
172	0.729	0.749	0.780	0.837	0.850
173	0.733	0.754	0.785	0.843	0.856
174	0.738	0.759	0.791	0.849	0.862
175	0.742	0.763	0.795	0.854	0.867
176	0.746	0.767	0.800	0.859	0.872
177	0.748	0.770	0.802	0.861	0.875
178	0.746	0.768	0.800	0.859	0.872
179	0.742	0.764	0.796	0.855	0.868

Table 1. (Continued)

β_1 (°) \ λ	0	0.8	0.9
(b) $b_1/a_1 = b_2/a_2 = 0.5$			
1	0.710	0.713	0.714
2	0.704	0.707	0.708
3	0.702	0.705	0.706
4	0.700	0.703	0.704
5	0.698	0.701	0.702
6	0.696	0.699	0.700
7	0.694	0.697	0.698
8	0.692	0.695	0.696
9	0.691	0.694	0.695
10	0.690	0.693	0.694
15	0.694	0.696	0.697
30	0.738	0.741	0.743
45	0.795	0.799	0.800
60	0.843	0.847	0.849
75	0.873	0.879	0.881
90	0.883	0.890	0.894
105	0.873	0.882	0.887
120	0.843	0.854	0.862
135	0.795	0.810	0.822
150	0.738	0.757	0.777
165	0.694	0.716	0.747
170	0.690	0.714	0.748
171	0.691	0.715	0.750
172	0.692	0.716	0.752
173	0.694	0.718	0.755
174	0.696	0.721	0.758
175	0.698	0.723	0.761
176	0.700	0.725	0.763
177	0.702	0.728	0.766
178	0.704	0.730	0.769
179	0.710	0.736	0.776

$$\gamma_i = \frac{F_{Ii}(\beta_i)}{F_{I0}(\beta)} \quad i = 1,2 \ , \tag{8}$$

where $F_{I0}(\beta)$ are the results for a single crack, $\lambda = 2a_1/d \rightarrow 0$, see Table 1.

The interaction factor γ_i is then normalized by $F_{I0}(\beta)$ for a single semi-elliptical crack. From Fig. 4, it is found that along the outside of crack 1, namely at $\beta_1 = 0 \sim 90°$, the interaction is less than 3 percent, even when $\lambda = 0.9$. When $\lambda = 0.667$, the interaction is less than about 3% even at $\beta_1 \cong 180°$. The interaction at $b/a = 0.5$ is smaller than the one at $b/a = 1$.

In the previous analysis, [5, 6], with Poisson's ratio $\nu = 0$, it was concluded that the interaction can be neglected when the two cracks are spaced in such a manner that their two closest points are separated by a distance exceeding the smaller crack's largest axis. Figure 4 indicates that the conclusion for $\nu = 0$ can be applied to the case when $\nu = 0.3$.

4.2
Two different cracks ($a_1 \geq a_2, b_1 \geq b_2$ in Fig. 1)

Figure 5 shows the values of γ_1 and γ_2 when $a_2/a_1 = 0.5$ is fix at a varying ligament distance εa_1. By decreasing the value of ε, the value of γ_1 increases locally in the region $120 \leq \beta_1 \leq 180°$; however, the value of γ_2 increases in the whole range. Although the γ_2 value is larger than the γ_1 value, the maximum SIF appears at a certain point, $\beta_1 = 177°$, of crack 1 because the size of crack 1 is larger. Along the outside region $\beta_1 = 0 \sim 90°$ of crack 1, the interaction can be neglected even when $\varepsilon = 0.25$.

Figures 6 and 7 give the values of γ_1 and γ_2 for fixed ligament distances, $\varepsilon = 0.5$ and $\varepsilon = 0.25$ respectively, with the varying value of a_2/a_1. From Figs. 4–7, it may be concluded that the effect of crack 2 on the maximum $K_I(\beta)$ appears at $\beta_1 = 177°$ of crack 1. It can be neglected if the two cracks are spaced in such a manner that their two closest points are separated by a distance exceeding the small crack's major diameter.

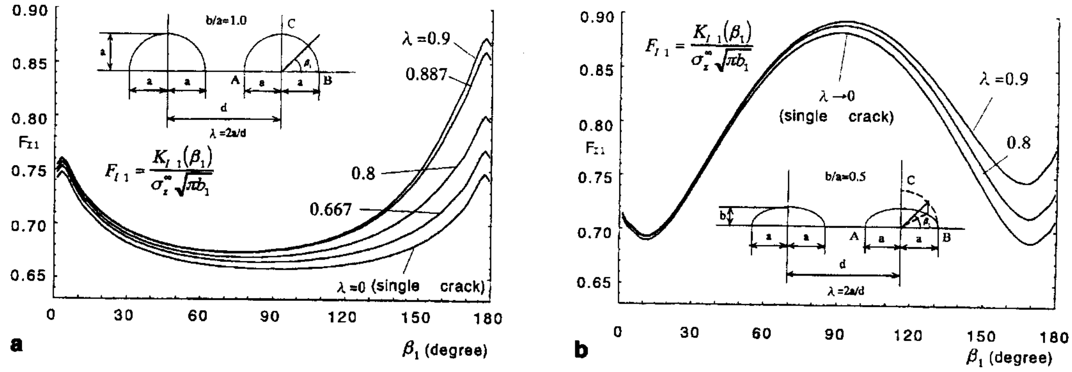

Fig. 3a, b. Variation of F_{Ii} of two identical semi-elliptical cracks **a** $b_1/a_1 = b_2/a_2 = 1$, **b** $b_1/a_1 = b_2/a_2 = 0.5$

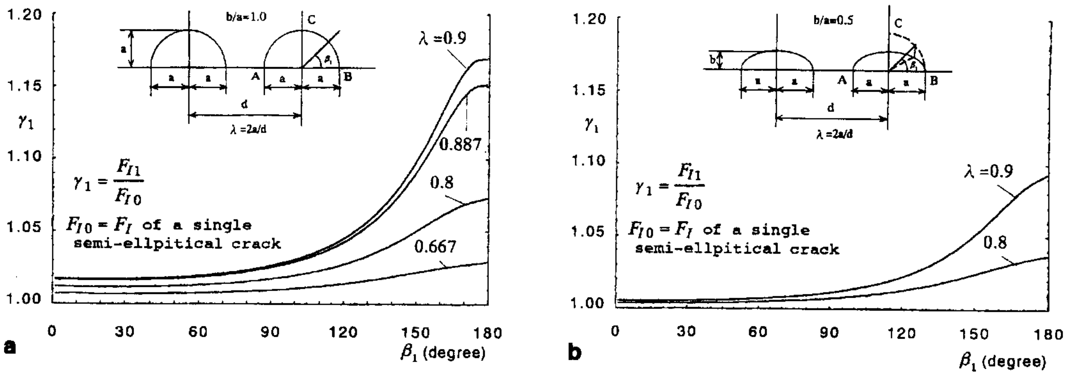

Fig. 4a, b. Variation of γ_1 of two identical semi-elliptical cracks **a** $b_1/a_1 = b_2/a_2 = 1$, **b** $b_1/a_1 = b_2/a_2 = 0.5$

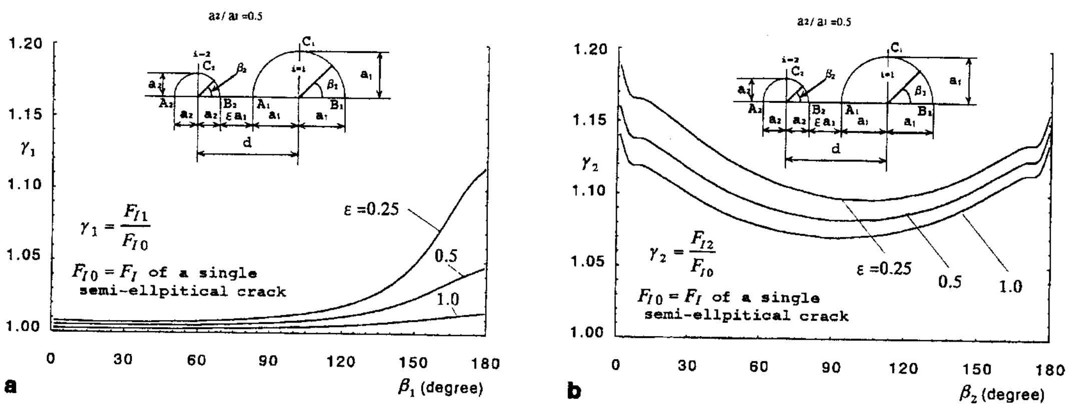

Fig. 5a, b. Variation of **a** γ_1 and **b** γ_2 of two semi-circular cracks when $a_2/a_1 = 0.5$

5
Conclusions

In this paper, a singular integral equation method is applied to calculate the variation of the SIF along the crack front of two co-planar semi-elliptical surface cracks. The conclusions can be made as follows:

(1) The unknown function of the body force density was approximated by the product of a fundamental density function and a weight function. The present method gives rapidly converging numerical results and smooth variations of the SIF along the crack front. The boundary condition was found to be satisfied within the error of 3×10^{-3} throughout the

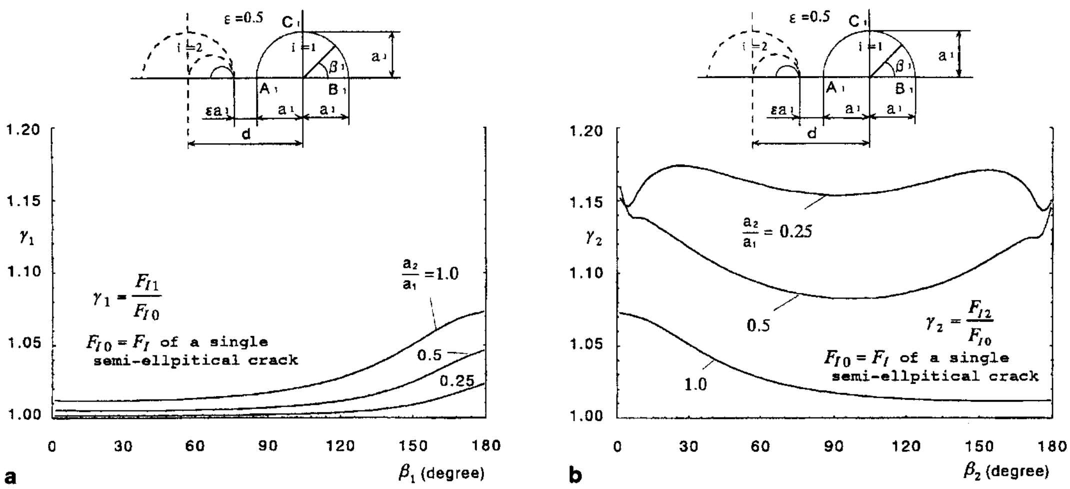

Fig. 6a, b. Variation of a γ_1 and b γ_2 of two different semi-circular cracks when $\varepsilon = 0.5$

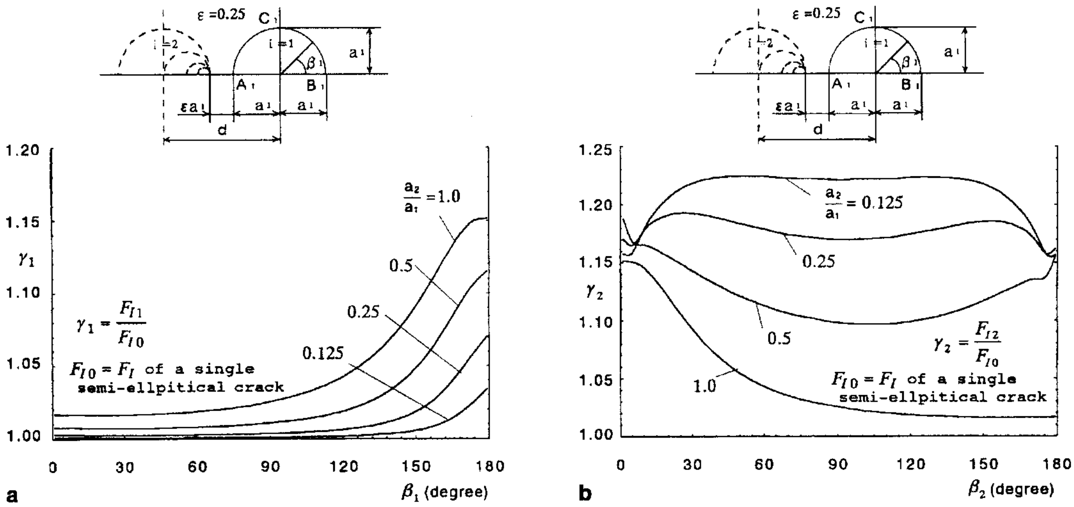

Fig. 7a, b. Variation of a γ_1 and b γ_2 of two semi-circular cracks when $\varepsilon = 0.25$

crack surface. The variations of the SIF of the semi-elliptical cracks were tabulated and charted.

(2) When the size of crack 1 is larger than the size of crack 2, the influence of crack 1 on crack 2 is larger than the opposite. However, since the size of crack 1 is larger, the maximum SIF appears at a certain point, $\beta_1 = 177°$, of crack 1. Along the outside of crack 1, that is for $\beta_1 = 0 \sim 90°$, the interaction can be negligible even if the cracks are close enough.

(3) The interaction between crack 1 and crack 2 can be negligible when the two cracks are spaced in such a manner that their two closest points are separated by a distance exceeding the small crack's major diameter.

References

1. **Miyata, H.; Kusumoto, K.:** On the stress intensity factor of three dimensional surface cracks. Transactions of JSME 45-391 (1979) 252–259 (in Japanese)
2. **Heath, B.J.; Grandt, Jr., A.F.:** Stress intensity factors for coalescing and single corner flaws along a hole bore in a plate. Eng. Fracture Mech. 19 (1984) 665–673
3. **Miyoshi, T.; Shiratori, M.; Tanabe, O.:** Stress intensity factors for surface cracks with arbitrary shapes in plate and shells. ASTM STP 868 (1985) 521–534
4. **Nishioka, T.; Furuya, Y.; Sana, Y.:** An alternative method for analysis of a group of interacting elliptical cracks in a infinite solids. Transactions of JSME 53-487 (1987) 537–543 (in Japanese)
5. **Murakami, Y.; Nisitani, H.:** Interacting two equal semi-elliptical surface cracks in tension. Transactions of JSME 47-415 (1981) 295–303 (in Japanese)

6. **Murakami, Y.; Nenat-Nasser, S.:** Interacting dissimilar semi-elliptical surface flaws under tension and bending. Eng. Fracture Mech. 16 (1982) 373–386
7. **Nisitani, H.:** The two-dimensional stress problem solved using an electric digital computer. J Japan Soc Mech Engineers, 70 (1967) 627–632 [Bull. Japan Soc of Mech Engineers 11 (1968) 14–23]
8. **Nisitani, H.; Murakami, Y.:** Stress intensity factor of an elliptical crack and semi-elliptical crack in plates subjected to tension. Int. J. Fracture 10 (1974) 353–368
9. **Murakami, Y. (ed.):** Stress intensity factors handbook 2, pp. 643–906. England, Pergamon 1987
10. **Murakami, Y. (ed.):** Stress intensity factors handbook 3, pp. 413–684, Japan Soc Mat Sci. England, Pergamon 1992
11. **Benthem, J.P.:** State of stress at the vertex of a quarter-infinite crack in a half-space. Int. J. Solids Struct. 13 (1977) 479–492
12. **Bazant, Z.P.; Estenssoro, L.F.:** Surface singularity and crack propagation. Int. J. Solids Struct. 15 (1979) 405–426
13. **Benthem, J.P.:** The quarter-infinite crack in a half space; alternative and additional solutions. Int. J. Solids Struct. 16 (1980) 119–130
14. **Noda, N.-A.; Miyoshi, S.:** Variation of stress intensity factor and crack opening displacement of semi-elliptical surface crack. Int. J. Fracture 75 (1996) 19–48
15. **Noda, N.-A.; Oda, K.:** Numerical solution of the singular integral equations in the crack analysis using the body force method. Int. J. Fracture 58 (1992) 285–304
16. **Hadamard, J.:** Lectures on Cauchy's problem in linear partial differential equations. Yale University Press, USA 1923
17. **Takakuda, H.; Koizumi, T.; Shibuya, T.:** On the solution of integral equations for crack problems. Transactions of the Japan Soc Mech Engineers 50A (1984) 1184–1192 (in Japanese)